eSim 2018
«BUILDING SIMULATION TO SUPPORT BUILDING SUSTAINABILITY»
IBPSA Canada
The Canadian Chapter of the International Building Performance Simulation Association
Le chapitre canadien de International Building Performance Simulation Association

An approach to virtual sensing of cooling systems using state-space inverse modelling and gradient descent

Jayson Bursill[1], William O'Brien[1], Ian Beausoleil-Morrison[1]

[1] Carleton University, Ottawa, Canada

Abstract: *Despite improvements in sensing quality and pricing, the installation of building automation integrated sensors often remains economically unjustifiable. Limited physical sensing in many buildings makes quantifying zone and room level energy flows challenging. A method to estimate cooling energy usage at a 15-minute resolution using state-space models and gradient descent parameter optimization is presented. Indoor air temperature, outdoor air temperature, and solar irradiation (with illuminance as a proxy) were used as inputs to inverse models of the indoor air temperature for estimating variable air volume cooling unit energy input. The cooling load was estimated for eight offices of an institutional building over a cooling season and maintained seasonal errors of 16% or less. The resultant parameters were found to not be universal, and varied significantly between offices within each zone. The presented methodology provides an approach for cooling quantification in previously unmetered buildings with applications to modelling and operations.*

Keywords: *virtual sensing, energy use estimation, building performance simulation*

Introduction

Virtual sensors utilize low cost measurements and mathematical models to estimate difficult to measure quantities (Li, Yu, & Braun, 2011; McDonald & Zmeureanu, 2015). The use of additional energy consumption information provided by virtual sensors in concert with other improvements in building operations from modified control algorithms can reduce total building energy use by up to 50% (Dong, O'Neill, & Li, 2014; Mathews, Botha, Arndt, & Malan, 2001; Tzempelikos & Athienitis, 2007). Numerous opportunities exist to reduce energy use in the current building stock, however, the absence or failure of physical sensors in many older buildings remains a barrier. Without feedback from physical sensors, it is difficult to quantify energy savings from conservation measures below the total building level. Virtual sensing has been commonplace in many other fields for decades (e.g., aerospace, automotive) (Li et al., 2011) and is garnering interest for buildings. Most work to date with building system virtual sensors has been focused on plant equipment (Schein, Bushby, Castro, & House, 2006; Seem, 2002; D. Yu, Li, & Yang, 2011; Y. Yu, Woradechjumroen, & Yu, 2014). While plant equipment comprises the larger portion of metered building energy consumption, zone level equipment comprises most of the physical equipment. Additionally, zone level equipment is often more difficult to diagnose, and acts as the conduit for transferring energy from the plant to the building occupants. The scale of zone equipment relative to plant equipment and the nominal costs of metering render direct metering at the zone level difficult to justify (under current equipment costs). Zone-based virtual sensors can provide useful energy data from zone level equipment for applications such as improving model calibration resolution, model predictive control (MPC) optimization functions, and fault detection (FD) benchmarking. Various approaches to FD have been explored for variable air volume (VAV) terminal units, including principle component analysis (Jin & Du, 2006; Qin & Wang, 2005), fuzzy logic (Liu & Dexter, 2001), autoregressive exogenous models (Yoshida, Kumar, & Morita, 2001), and artificial neural networks (Fan, Du, Jin, Yang, & Guo, 2010). A gap identified in modern FD analysis for VAV terminal systems was the presence of outputs that provide contextual data for system control and visualization. While the previously analyzed techniques can provide black-box results, the contextual data are limited. The need for a compromising approach that is both computationally simple and conducive to quantitative zonal comparison was identified.

Conversely, contemporary VAV terminal unit control and subsequent modelling work is focused on detailed analysis of geometric and thermal properties. A dichotomy between first principles models that require consistent and direct measurements (Salsbury, 1998; Wang & Jin, 2000; Zaheer-Uddin & Zheng, 1994) and empirical models with limited contextual data (Chen & Deng, 2006; Cherem-Pereira & Mendes, 2012; Xu, Wang, Sun, & Xiao, 2009) exists, where tuning for different conditioned spaces in the absence of permanent physical sensors is cumbersome. Resultantly, zone level energy use estimation is uncommon in commercial buildings. This renders comparison and system management at the zone level difficult.

The study presented in this paper attempts to provide an approach to estimating cooling energy consumption of spaces with linear parameter state-space models of VAV zone level terminal unit cooling output power (averaged over 15 minutes) utilizing only data from eight offices and plant level air handling units. The use of standard building automation system (BAS) sensors in this study distinguishes virtual sensors from empirical models and direct measurement-derived approaches. Measurement-derived cooling energy consumption estimates are

ISBN 978-2-921145-88-6

obtained from direct measurements of the VAV box outlet (dock) temperature, VAV unit flow, and room temperature. The virtual sensor for cooling energy is presented as a state-space model initially trained for room temperature prediction. The model is then rearranged to use current room temperature, past room temperature, and illuminance data to estimate the previous time step cooling energy consumption. Model validation consists of comparing the results of the state-space models with the measurement derived cooling energy estimates. Models that produce results with mean absolute error (MAE) within the uncertainty of the monitoring equipment can be inferred as acceptably accurate and applicable for VAV cooling energy estimation.

Methodology

Measurement Derived VAV Cooling Estimation

The virtual sensor development proposed in this paper requires an estimate of the desired output value to train the linear parameter state-space models. Many modern VAV control systems will measure temperatures at the air handling unit outlet, VAV box outlet, and conditioned space. Regulation of the air damper within the VAV box requires a flow or pressure sensor (or another proxy) for closed loop control. Humidity sensors are currently uncommon at the space level, and the lack of accuracy observed in the facility studied is prohibitive to accurate estimation of latent energy at the zone level. Further, the sensible cooling loads were found to be dominant, where sensible heat fractions of 0.6 – 0.9 were observed at the coil of the air handling unit over the cooling season for the zones served. Latent cooling was not unsubstantial, and could be the focus of future work in the presence of improved humidity sensing. As a result of the sensor accuracy limitation, only sensible loads were estimated in this study.

The zone level cooling system consists of a VAV terminal unit to regulate airflow that serves four offices. Airflow was provided from a fan at the air handling unit where air is initially cooled to a temperature that meets the largest zone demand. The airflow to each office was assumed to be an equal division of the zone airflow measured at the VAV box. When cooling is required, airflow is modulated via the VAV zone level damper to allow the space to achieve a setpoint as defined by the occupant. The setpoint could vary from 18°C to 27°C as defined by each office thermostat. The VAV box also provides the outdoor air requirement. Data was sampled at 15-minute intervals for analog values and upon state changes for binary inputs. The measurement derived estimation only used analog values. Binary values from passive infrared occupancy sensors were utilized to infer thermal loads from occupants and equipment. Flows for each office were assumed to be an equal division of the zone flow (verified to be true within ±10% of the assumed room airflow). All offices are oriented facing 30 degrees North of West.

Assumed space properties included negligible thermal short-circuiting and steady-state VAV units. All thermal storage was attributed to the single node room model. For context, the external wall glazing ratio was estimated to be 0.3 (with one of four walls being external), and a window U-factor of 2 W/m^2-K and solar heat gain coefficient of 0.6 were assumed in previous detailed model sizing runs.

An initial dynamic heat balance is introduced as a first order single node temperature model of each office in Equation 1, where T is temperature, q is net heat flow, u_4 is the outdoor air temperature, R is the thermal resistance between the indoor and outdoor nodes, C is the thermal capacitance of the indoor node, t is the time index, i is the indoor node index, and o is the outdoor node index (Athienitis, 1994). This equation is later adapted to a similarly structured data-driven state-space approach in Equation 3 and Equation 4. A two node model was also investigated, but only yielded a 1.4% reduction in MAE between the measurement derived and virtual cooling values.

$$T_i(t+1) = \frac{\Delta t}{C_i}\left(\left(\frac{u_4(t) - T_i(t)}{R_{i,o}}\right) + q_i(t)\right) + T_i(t) \qquad (1)$$

A diagram of the different inputs of interest that are used in this study, and their respective sensor location and variable name is provided Figure 1. A summary of the available sensors is provided in Table 1. Notably, some spaces do not measure VAV box outlet temperature and would limit a measurement derived approach without the addition of standalone equipment for initial virtual sensor calibration.

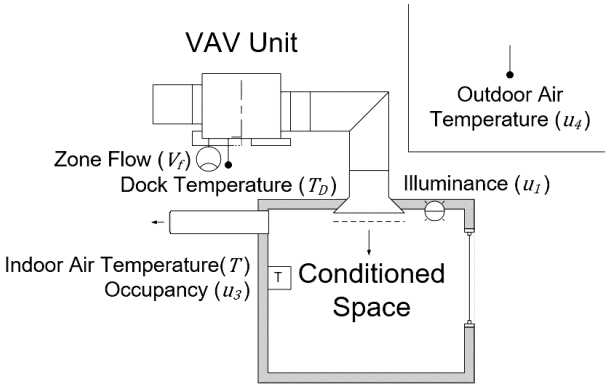

Figure 1. Sensor and airflow diagram for VAV air conditioning system

Table 1: Sensor schedule for Figure 1

Measured Quantity	Sensor
Zone Flow (V_f)	Differential Pressure Transducer
Indoor Air Temperature (T)	10 kOhm Thermistor
VAV Box Outlet Temperature (T_D)	4-20 mA Resistance Temperature Detector
Illuminance (u_1)	Photodiode
Occupancy (u_3)	Passive Infrared
Outdoor Air Temperature (u_4)	10 kOhm Thermistor

ISBN 978-2-921145-88-6

Equation 2 was used to estimate the sample average heat transfer rate to the conditioned space using a measurement-derived first principles based approach for sensible cooling. Air and surface temperatures were assumed to be equal to facilitate a single node model. The virtual cooling energy consumption for the space could be calculated using the VAV box outlet temperature, $T_D(t)$, room air temperature, $T(t)$, air specific heat, c_{pa}, air density, ρ_a, and room air flow rate (in the form of the total zone flow rate divided by the number of offices), V_f. The air temperatures and flow rates were obtained from the BAS serving the observed room, and the air thermo-physical properties were inferred from average VAV box air temperatures.

$$Q(t) = V_f \rho_a c_{pa}\big(T(t) - T_D(t)\big) \quad (2)$$

Linear Parameter State-space Model

An alternate (and indirect) approach to estimating the cooling energy consumption of each office involved training a linear time-invariant state-space model to the measurement derived estimates. A linear time-variant model could provide flexibility to accommodate transient space properties, but would require recursive training (contrary to the intent of the proposed virtual sensors). The heat balance introduced in Equation 1 can be represented in the discrete canonical state-space form of Equation 3. The MATLAB System Identification Toolbox (Ljung, 1995) was used to obtain the matrices A and B of Equation 3 for each office, where T is the state vector and u is the input vector with respect to time. Training was executed with one week of measured data from temperature states T (°C), illuminance $u_1(t)$ (lux), VAV cooling energy consumption rate, $u_2(t)$ (W), occupancy state $u_3(t)$ (binary), and indoor to outdoor temperature differential $u_4(t)$ (°C) for time t, in the form of Equation 4a. Equation 4a was based on the recommendations of previous work in linear state-space model room temperature estimation, where illuminance is used as a proxy for solar gains (Gunay, Bursill, Huchuk, O'Brien, & Beausoleil-Morrison, 2014). Full stability for 15-minute time steps was assumed (and verified by A values an order of magnitude smaller than the sample interval).

$$T(t+1) = AT(t) + Bu(t) \quad (3)$$

The state-space equation expansion in Equation 4a was algebraically rearranged to Equation 4b to estimate the measurement-derived VAV cooling input for the previous time step. Due to the change in model focus from temperature state prediction to cooling input estimation, linear time-invariant parameters vectors A and B were adjusted to improve estimation accuracy. A gradient descent technique was applied to the training data to find the new near-optimal values for cooling energy estimation (where the A and B values from the temperature prediction model as a starting point) in the format shown in Equation 4b and Equation 4c (Lasdon, Fox, & Ratner, 1974).

Through sensitivity analysis it was found that the occupancy state and indoor to outdoor temperature differential had lower effects on the VAV cooling input by an order of magnitude than the other inputs and states, and as an approximation could be neglected for the offices analyzed. This simplified the model and training process, but limited the ability for the model to react to occupant disturbances and extreme weather conditions in other buildings. The model selected from the parameter optimization and sensitivity analysis process to approximate previous time step VAV cooling input is provided in Equation 4c. The target time is adjusted from $t+1$ to $t-1$ to satisfy the requirement of $T(t)$ in equation 4c as a representation of $T(t+1)$ from Equation 4a. A graphical representation of the model reduction is provided in Figure 2, where a thermal resistance and capacitance were initially assumed to act in conjunction with heat inputs for the first order thermal model. After the sensitivity analysis, it was determined that only an aggregate capacitance and two heat inputs were required. The aggregate thermal capacitance is a factor of B_1 and B_2, but is not physically significant with respect to the scope of this work and was not explicitly calculated. However, the relative values of A, B_1, and B_2 can provide contextual data regarding the influence of thermal mass, solar gains, and VAV cooling on each office respectively.

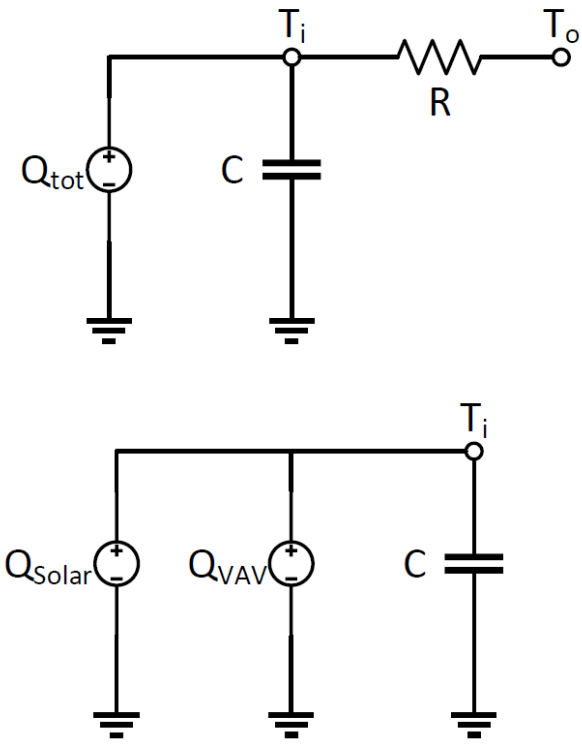

Figure 2: (Top) Initial generic first order lumped thermal resistance and capacitance model. (Bottom) First order lumped capacitance model selected from sensitivity analysis

ISBN 978-2-921145-88-6

$$T(t+1) = AT(t) + B_1u_1(t) + B_2u_2(t) + B_3u_3(t) + B_4u_4(t) \quad (4a)$$

$$u_2(t-1) = \frac{1}{B_2}\big(T(t) - AT(t-1) - B_1u_1(t-1) - B_3u_3(t-1) - B_4u_4(t-1)\big) \quad (4b)$$

$$Q(t-1) \approx u_2(t-1) = \frac{1}{B_2}\big(T(t) - AT(t-1) - B_1u_1(t-1)\big) \quad (4c)$$

Instrumentation Uncertainty

The estimated range of model error was determined using experimental uncertainty derived from physical sensor data. A model was considered acceptable when both MAE and RMSE were within the VAV cooling output uncertainty. This uncertainty was obtained using a separation of variables approach as presented in Equation 5. Partial derivatives were taken for each Equation 2 input to satisfy Equation 5, where s_Q is the bias error of the measurement derived cooling and x_i is the bias error for each respective input.

$$\Delta s_Q^2 = \sum_{i=1}^{n}\left(\frac{\partial Q}{\partial x}\right)^2 \Delta x_i^2 \quad (5)$$

A static value of bias error of cooling energy was chosen from the highest observed flow rate and temperature differential to encompass a conservative estimation of uncertainty. Property values and their individual bias errors were taken from the literature (Incropera, Lavine, Bergman, & DeWitt, 2007), and input measurement maximum values and instrumental bias errors were obtained from data over the full cooling season and catalog information respectively. A summary of the values used for this calculation is provided in Table 2. Uncertainty was calculated as a root mean square of the bias error and precision error. The precision error was found to be negligible with respect to the bias error. Using this approach, an uncertainty of 700 W was obtained.

Table 2: Input average values and bias errors for first principles estimate

	Average Value	Instrument Bias Error
V_f (m^3/s)	0.250	2.1x10^{-2}
ρ_a (kg/m^3)	1.225	0.1125
c_{pa} (J/kg-K)	1000	5
$T(t) - T_D(t)$ (°C)	5.0	0.4

Cooling output uncertainty is shown over 12 hours of measurement derived cooling estimation in Figure 3. At low values, the measurement uncertainty becomes a significant portion of the total reading, while at higher values it is within reasonable bounds. Significant uncertainty can be attributed to the air flow bias error, which is 1% of full scale (8.4% of the average reading). Calibration of the flow measuring equipment during building commissioning would likely mitigate the uncertainty observed in this analysis. However, the effects of sensor calibration are difficult to quantify for experimental purposes. Additionally, the room level division of zone level airflow could induce an uncertainty (due to difference in balancing and duct lengths) of up to 5 L/s as observed by spot measurements.

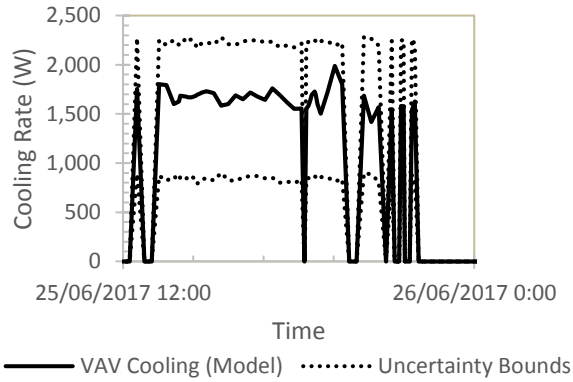

Figure 3: VAV cooling virtual sensor estimation with uncertainty bounds of measurement derived VAV cooling estimation for one office over one afternoon

Results and Discussion

The resulting algebraically rearranged state-space model errors were within the uncertainty bounds of the measurement derived estimates of office cooling energy. Mean absolute error (MAE) and coefficient of variation (CoV) as defined in Equation 6 were within instrumentation uncertainty and a reasonable portion of the average value for each office respectively. This is verified in Table 3, where the MAE of each office cooling energy estimate is within the instrumentation uncertainty of 700 W, and the CoV was 22-26%. MAE was obtained only for measurements where the cooling system was active because the virtual cooling estimates were zeroed when the system was inactive. A comparison of the measurement derived (measured) and virtual (model) cooling energy is provided in Figure 5. All spaces modelled demonstrated conformity while the cooling was temperature driven, while there was additional discrepancy during solar driven peaks. The MAE consistently remained between 440 W and 488 W for each room. Figure 4 shows the lag between solar peaks and indoor air temperature peaks, which were observed to range from two to four hours (in comparison to the 15-minute model time step). This is a source of error from the use of a one node model that could be reduced by using a model with multiple nodes to include thermal information from additional previous time steps. While a higher order model could achieve more accurate results, it would induce complexity with diminishing accuracy improvement. A two node model was observed to only reduce MAE by 1.4%.

ISBN 978-2-921145-88-6

$$CoV = \frac{MAE}{Average} \quad (6)$$

Table 3: MAE for linear time invariant VAV output models compared to measurement derived values

Room	MAE (W)	CoV
1	462	24%
2	440	24%
3	462	24%
4	486	26%
5	460	22%
6	488	24%
7	455	22%
8	462	23%

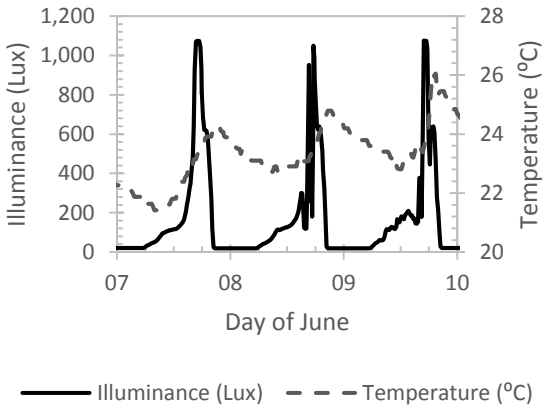

Figure 4: Solar proxy (lux) and indoor air temperature for one office over two days

Model error was quantified differently for training than evaluation. To further penalize outliers, root mean square error (RMSE) was minimized during parameter gradient descent. Final assessment used the previously presented MAE, while RMSE was used in its place to assess model fit. Using MAE in place of RMSE for training would yield a model less responsive to disturbances and more centered about the average cooling value.

A goal of this analysis was to determine if a universal linear parameter model could be used to approximate room parameters with no training or knowledge of the system. If this could be proven within a cooling system or even individual zone, reduced sensor requirements could be feasible for rough cooling energy estimates and basic control. This was not the case, as shown in Table 4. The standard deviation of parameter values within the office block studied (broken into two zones of four offices each) was greater than the average value for the input parameters B_1, and B_2 and still high for the state parameter, A. However, the relative parameter values could be interpreted contextually to determine some characteristics of the space. Offices with higher solar parameter (B_1) values were observed to have more window obstruction, rendering cooling energy increase more sensitive to proportionally small illuminance input changes. Conversely, because the algebraic rearrangement of the state-space model is divided by the VAV parameter (B_2) a larger value is proportional to a higher thermal mass.

Relative parameter values could be used to categorize spaces into similar types as proposed in previous work (Kim & Braun, 2015; Shi & O'Brien), and these categories of spaces could be assigned archetypal parameter values. However, this approach would be qualitative and involve heuristics in the absence of physical sensors, thus reducing reliability.

Parameters that were removed due to lack of cooling sensitivity in this application may be non-negligible in other buildings or applications. As such, they were introduced in this paper but not used in the later stages of simulation. A more diverse set of offices would be required to determine if the input assumptions in the proposed model are applicable for all (or most) spaces.

Measurement derived cooling estimates did not vary significantly between spaces within a zone (less than 5%) and can be seen in Figure 6 (where offices served by the same zone are grouped). This is a product of inter-zonal flow variability. Due to the flow being assumed equal between all four spaces within the two zones, one space could be used as an approximation for all within the zone under the assumption that adjacent room temperatures are similar. The same is not true for different zones, where differences in flow produce significantly different cooling energy consumption.

A portion of uncertainty that was previously introduced but not discussed was the splitting of the measured airflow of each VAV unit among the four served spaces. An average flow error of 8% was observed between spot measurements (capture hood) and BAS sensor values. This was used as an upper limit on the error generated from dividing zone flow between the served offices. From spot measurements the highest error was observed at the maximum flow rate. This was justified because calibration and balancing is typically executed about a traditional operating point where accuracy is maintained.

ISBN 978-2-921145-88-6

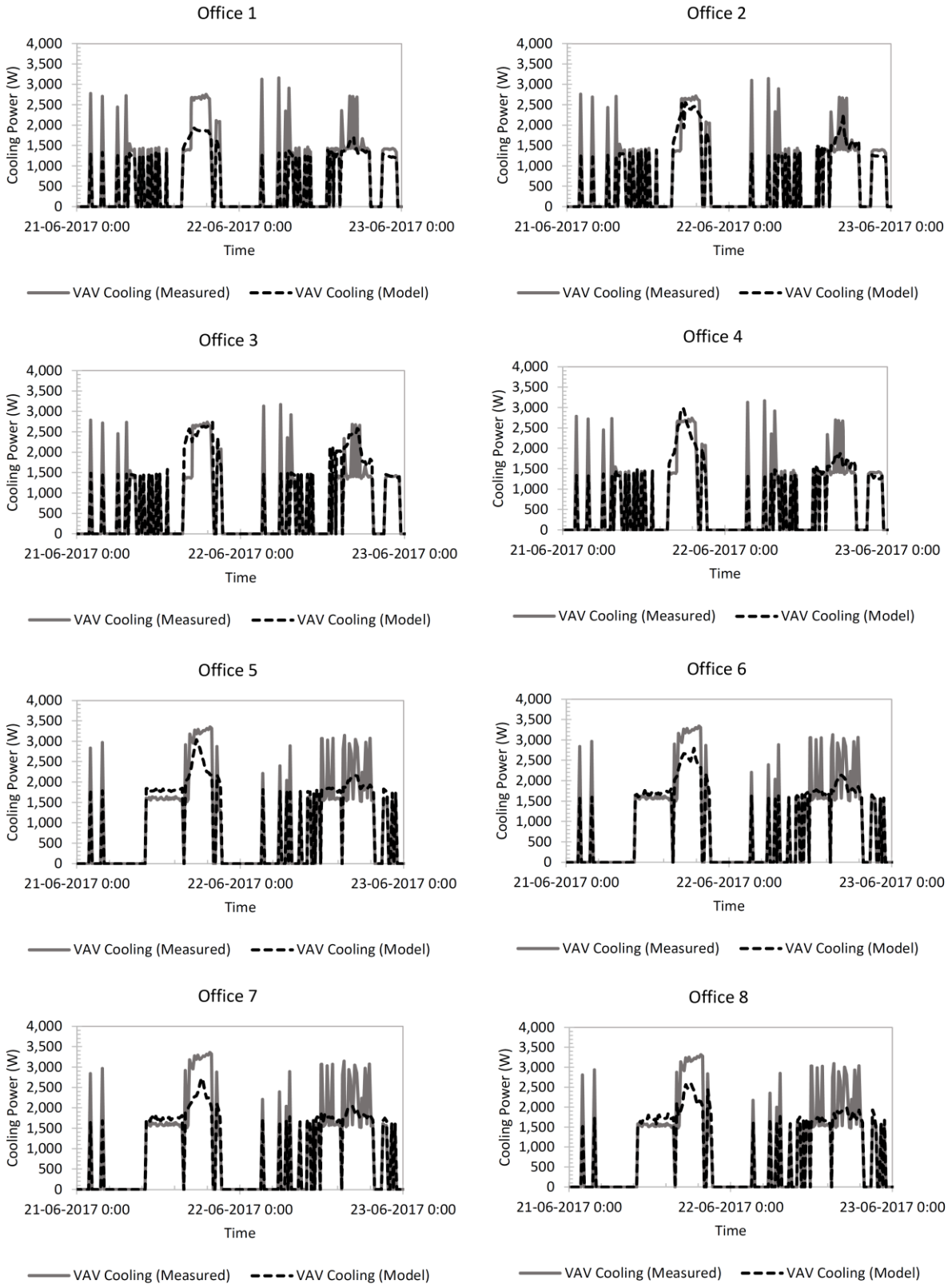

Figure 5: Comparison of model estimated (virtual) and measurement derived cooling energy averaged over 15-minute sample intervals for all eight offices

ISBN 978-2-921145-88-6

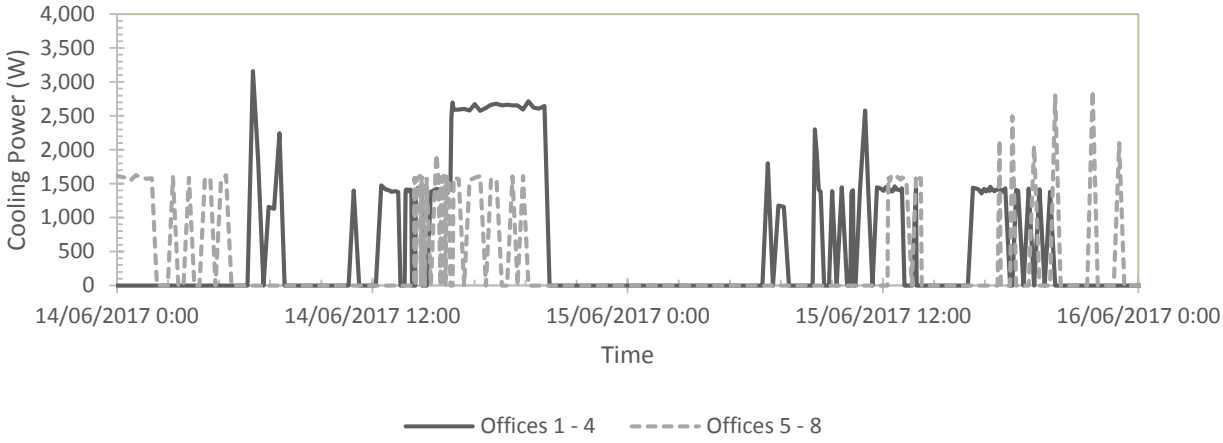

Figure 6: Measurement derived cooling values for the two office zones studied over two days

Table 4: Parameter estimates for the office block

Room	Parameter		
	A – (unitless)	B1 - Solar (Degree/lux)	B2 - VAV (Degree/W)
1	1.38	0.0014	0.007
2	2.50	0.0041	0.029
3	2.47	0.1373	0.024
4	1.15	0.0102	0.003
5	1.78	0.0189	0.010
6	1.42	0.0182	0.006
7	1.14	0.0068	0.002
8	1.08	0.0012	0.001
Average	1.61	0.0247	0.010
Standard Deviation	0.58	0.0460	0.011
Coefficient of Variation	36%	186%	103%

Cooling energy consumption as defined in this paper is limited as an average of energy over a 15-minute interval. Digital values from the BAS were event based, while analog values were sampled every 15 minutes (as used in the discrete state-space models). Higher sampling frequency was not found to improve model accuracy significantly over the whole day.

The daily cooling energy was calculated using both the measurement derived and linear parameter model approaches, and compared over the entire cooling season. Measurement-derived and virtual-sensed daily cooling energy for a sample office (Office 8) is shown in Figure 7. While the peaks are often under estimated, the error for the cooling season remained relatively small (within 16% for all offices) over the whole cooling season as shown in Table 5.

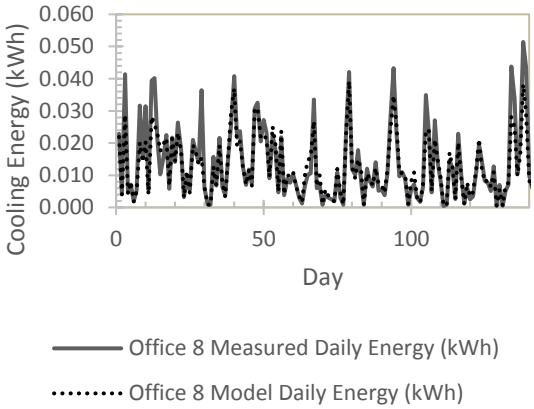

Figure 7: Measurement derived and virtual sensor daily cooling energy estimates for one office over the cooling season

Table 5: Cooling energy estimated over the cooling season

	Cooling Season Measured Energy (GJ)	Cooling Season Model Energy (GJ)	Seasonal Error (%)
Office 1	5.1	4.31	-16%
Office 2	5.05	4.46	-12%
Office 3	5.11	4.72	-8%
Office 4	5.11	4.85	-5%
Office 5	7.03	6.78	-4%
Office 6	6.99	6.22	-11%
Office 7	7.03	6.51	-7%
Office 8	6.91	6.31	-9%

ISBN 978-2-921145-88-6

Instrumentation uncertainty will likely be an ongoing challenge with the application of virtual sensors. Utility grade accuracy is usually not achieved by typical BAS terminal sensors, and degradation is almost certain with the volume of sensors present in most commercial buildings. This could be an opportunity if virtual sensor models were used to detect sensor failure or performance degradation over time. This study only looked at time invariant models over one cooling season. More work is required to determine the parameter evolution with respect to time using time variant models to confirm the validity of this assumption over several cooling seasons.

Future work in state-space model based virtual sensors to build upon the work presented in this paper should include:

- Higher order models for handling solar gains.
- Other sensor inputs to determine the most suitable model for each space.
- Weather station solar data to improve solar gain estimation accuracy.
- Other terminal applications such as heating, casual gains, etc.

The same methodology introduced in this paper could be applied to other linearized heat transfer modes within buildings. Immediately apparent opportunities could be forced air heating systems and other non-radiant terminal heating and cooling modes.

Conclusion

Virtual sensing can estimate HVAC inputs to buildings with indirect sensing and has applications in energy use estimation and fault detection. The flexibility to adapt to available sensors can be useful in model predictive control schemes to estimate cost function values in real time using previously acquired input values. Space to space parameter variation prohibits universal parameter values, but zone grouping could improve the accuracy of generalized values and heuristics. The approach utilized in this virtual cooling study could also be applied to other terminal input modes in buildings if the superposition and linearization assumptions remain accurate.

The goal of terminal unit virtual sensing is to provide energy use and comparison data to control algorithms and building owners while minimizing physical sensing requirements. A software based approach is both cost effective and comparatively easy to implement in the unified BACnet building automation protocol. MAE for all office virtual sensors (440 – 488 W) over the entire cooling season remained within the measurement derived uncertainty of 700 W. Further, the maximum seasonal error of estimated cooling energy was 16%, indicating reliability over longer term summations. The results of this study demonstrate that there is promise in using LTI state-space room models to virtually meter terminal heating, ventilating, and air conditioning equipment when physical sensing is limited.

References

Athienitis, A. (1994). Building thermal analysis. *Electronic Book Mathcad, MathSoft, Boston, USA*.

Chen, W., & Deng, S. (2006). Development of a dynamic model for a DX VAV air conditioning system. *Energy conversion and management, 47*(18), 2900-2924.

Cherem-Pereira, G., & Mendes, N. (2012). Empirical modeling of room air conditioners for building energy analysis. *Energy and Buildings, 47*, 19-26. doi: 10.1016/j.enbuild.2011.11.012

Dong, B., O'Neill, Z., & Li, Z. (2014). A BIM-enabled information infrastructure for building energy Fault Detection and Diagnostics. *Automation in Construction, 44*, 197-211.

Fan, B., Du, Z., Jin, X., Yang, X., & Guo, Y. (2010). A hybrid FDD strategy for local system of AHU based on artificial neural network and wavelet analysis. *Building and environment, 45*(12), 2698-2708.

Gunay, H. B., Bursill, J., Huchuk, B., O'Brien, W., & Beausoleil-Morrison, I. (2014). Shortest-prediction-horizon model-based predictive control for individual offices. *Building and Environment, 82*, 408-419. doi: 10.1016/j.buildenv.2014.09.011

Incropera, F. P., Lavine, A. S., Bergman, T. L., & DeWitt, D. P. (2007). *Fundamentals of heat and mass transfer*: Wiley.

Jin, X., & Du, Z. (2006). Fault tolerant control of outdoor air and AHU supply air temperature in VAV air conditioning systems using PCA method. *Applied Thermal Engineering, 26*(11), 1226-1237.

Kim, D., & Braun, J. E. (2015). A general approach for generating reduced-order models for large multi-zone buildings. *Journal of Building Performance Simulation, 8*(6), 435-448.

Lasdon, L. S., Fox, R. L., & Ratner, M. W. (1974). Nonlinear optimization using the generalized reduced gradient method. *Revue française d'automatique, informatique, recherche opérationnelle. Recherche opérationnelle, 8*(V3), 73-103.

Li, H., Yu, D., & Braun, J. E. (2011). A review of virtual sensing technology and application in building systems. *HVAC&R Research, 17*(5), 619-645.

Liu, X.-F., & Dexter, A. (2001). Fault-tolerant supervisory control of VAV air-conditioning systems. *Energy and Buildings, 33*(4), 379-389.

Ljung, L. (1995). System Identification Toolbox for use with MATLAB.

Mathews, E., Botha, C., Arndt, D., & Malan, A. (2001). HVAC control strategies to enhance comfort and minimise energy usage. *Energy and Buildings, 33*(8), 853-863.

McDonald, E., & Zmeureanu, R. (2015). Development and testing of a virtual flow meter tool to

ISBN 978-2-921145-88-6

monitor the performance of cooling plants. *Energy Procedia, 78*, 1129-1134.

Qin, J., & Wang, S. (2005). A fault detection and diagnosis strategy of VAV air-conditioning systems for improved energy and control performances. *Energy and Buildings, 37*(10), 1035-1048.

Salsbury, T. (1998). A temperature controller for VAV air-handling units based on simplified physical models. *HVAC&R Research, 4*(3), 265-279.

Schein, J., Bushby, S. T., Castro, N. S., & House, J. M. (2006). A rule-based fault detection method for air handling units. *Energy and Buildings, 38*(12), 1485-1492.

Seem, J. E. (2002). Model based economizer control of an air handling unit: Google Patents.

Shi, Z., & O'Brien, W. Building Energy Model Reduction using Principal Component Analysis and Affinity Propagation Clustering of Thermal Zones.

Tzempelikos, A., & Athienitis, A. K. (2007). The impact of shading design and control on building cooling and lighting demand. *Solar Energy, 81*(3), 369-382.

Wang, S., & Jin, X. (2000). Model-based optimal control of VAV air-conditioning system using genetic algorithm. *Building and environment, 35*(6), 471-487.

Xu, X., Wang, S., Sun, Z., & Xiao, F. (2009). A model-based optimal ventilation control strategy of multi-zone VAV air-conditioning systems. *Applied Thermal Engineering, 29*(1), 91-104.

Yoshida, H., Kumar, S., & Morita, Y. (2001). Online fault detection and diagnosis in VAV air handling unit by RARX modeling. *Energy and Buildings, 33*(4), 391-401.

Yu, D., Li, H., & Yang, M. (2011). A virtual supply airflow rate meter for rooftop air-conditioning units. *Building and Environment, 46*(6), 1292-1302.

Yu, Y., Woradechjumroen, D., & Yu, D. (2014). A review of fault detection and diagnosis methodologies on air-handling units. *Energy and Buildings, 82*, 550-562.

Zaheer-Uddin, M., & Zheng, G. (1994). A VAV system model for simulation of energy management control functions: off normal operation and duty cycling. *Energy conversion and management, 35*(11), 917-931.

ISBN 978-2-921145-88-6